SCENARIO BASED GROUND MOTION SIMULATIONS FOR ASSESSING THE SEISMIC HAZARD IN İZMIR, TURKEY

L.W. Bjerrum[1] and K. Atakan[2]

[1] *MSc., Dept. of Earth Science, University of Bergen, Bergen .Norway*
[2] *Professor, Dept. of Earth Science, University of Bergen, Bergen. Norway*
Email: louise.bjerrum@geo.uib.no, kuvvet.atakan@geo.uib.no

ABSTRACT :

Collision of the Arabian and African plates with Eurasia forces the Anatolian micro-plate to move west-wards. In the Aegean Sea, the Anatolian micro-plate rotates counter-clockwise and extends due to the subduction zone along the Hellenic Arc. This deformation results in reactivation of faults on the west coast of Turkey, which results in destructive earthquakes. İzmir, the third largest city in Turkey, has been destroyed by (large) earthquakes several times in recent history, latest in 1778. In this study, a deterministic seismic hazard analysis is conducted based on ground motion simulations for nine different earthquake rupture scenarios for recognized faults in the area surrounding İzmir. The method adopted is a hybrid broad-band ground motion simulation technique, which has previously been validated. The earthquake scenarios are based on existing knowledge of source parameters, local as well as regional. Among the various faults surrounding İzmir, the largest peak ground motions are associated with two faults, the İzmir fault (normal) which lies underneath the city and the Tuzla fault (strike-slip) which lies southwest of the city. The results indicate that a rupture on the 42 kilometer long İzmir fault can produce ground acceleration as high as 0.3 g on bedrock level in the center of İzmir. Considering the site effect potential in the area, this value needs to be treated as the lower threshold. The simulation results indicate that the historic events that have caused severe destruction in İzmir most likely have occurred on either the İzmir or the Tuzla faults. Furthermore the attenuation of the simulated ground motions agrees well with empirical relations as far as peak ground accelerations are concerned.

KEYWORDS: Fault models, Seismic hazard, Earthquake scenarios, Western Turkey, Strong ground motion simulations

1. INTRODUCTION

The Aegean-Anatolian region is one of the most seismically and tectonically active areas within Europe and is characterized by significant seismic hazard. Extensive information exists on active faults based on high-resolution GPS datasets covering the Aegean and Anatolian regions as well as from regional and local geological studies. The GPS data show that the Anatolian micro-plate moves westwards with most deformation occurring along the well known North Anatolian Fault Zone. Various interpretations of the GPS data exist; dividing the region into a number of micro-plates separated by relatively narrow zones that accommodate most of the tectonic deformation (Nyst and Thatcher, 2004).

The active deformation in western Anatolia results in reactivation of various fault systems in the region, as destructive earthquakes have demonstrated in geological and historical times. During recent history there have been three catastrophic earthquakes in İzmir, Turkey. These earthquakes took place with approximately 50 years intervals; the latest occurring in 1778 (Ambraseys and Finkel, 1995; Papazachos and Papazachou, 1997; Papazachos, et al., 1997).

Numerical ground motion simulation methods using earthquake scenarios are now currently being applied for estimating the seismic hazard in regions where the hazard is controlled by a nearby large fault. İzmir is exposed to significant hazard due to its proximity to several active faults. This study aims to quantify the ground motion distributions as a result of earthquake rupture along the well-defined faults near İzmir. In this study seismic hazard in the area is assessed deterministically based on nine different earthquake scenarios on active faults located around the city of İzmir. The methodology used is based on a hybrid broad-band ground motion

simulation technique already applied in Tottori, Japan and Istanbul, Turkey with success (Pulido and Kubo, 2004; Pulido, et al., 2004; Sørensen, et al., 2007). The source complexity is represented using multi-asperity models with various parameters defining the physical properties of the slip during the scenario earthquake rupture. Input models are based on the characteristics of both the source (fault dimensions, geometry, mechanism, size and location of asperities and their parameters) and the path (seismic velocities and attenuation in the crust). Comparison of the results from the ground motion simulation gives new insights on the critical faults that control the seismic hazard in İzmir.

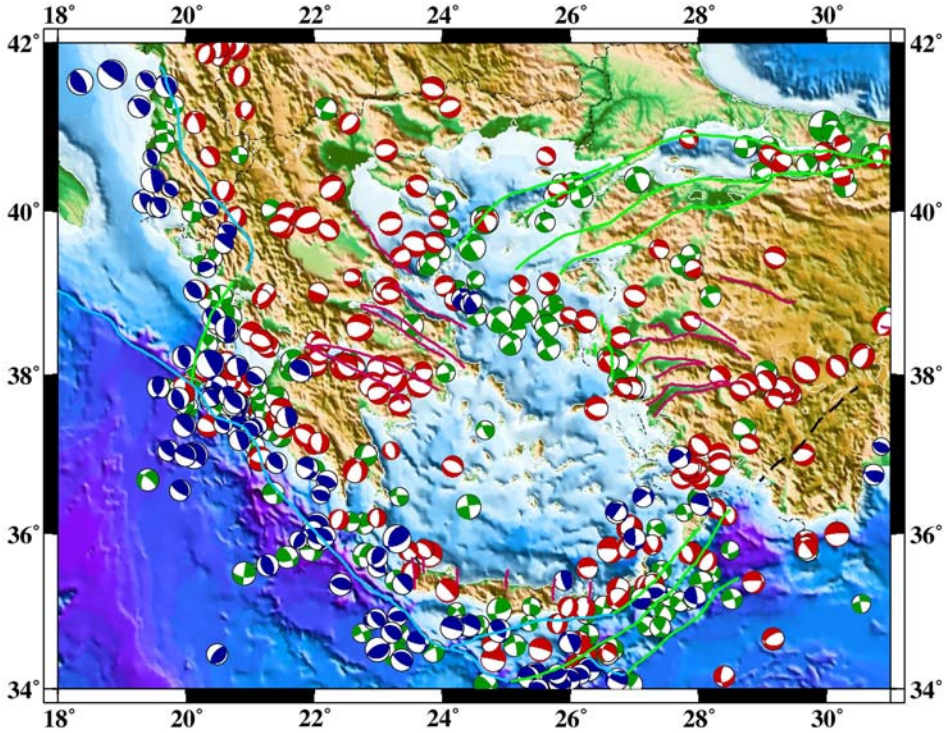

Figure 1 Active faults and earthquake focal mechanisms in the Aegean region. The fault plane solutions are compiled from the INGV, USGS and Global CMT moment tensor solution databases.

2. SEISMOTECTONIC BACKGROUND AND METHODOLOGY

The large-scale deformation of the tectonics in the Aegean-Anatolian region is dominated by the collision of the African and Arabian plates with Eurasia. The collision of the Arabian plate with the Eurasian plate causes a westward migration of the Anatolian block, which is accommodated by two large right and left lateral strike-slip faults; North and East Anatolian Fault zones respectively. In the west the African plate is subducted underneath the Aegean Sea along the Hellenic Arc. The focal mechanisms of the earthquakes in the Northern Aegean Sea are mainly strike-slip, which is a result of the westward migration of the Anatolian plate. Along the Hellenic Arc and northwards along the continental collision zone between northwestern Greece and Albania with the Apulia-Adriatic platform there are thrust faulting earthquakes. Normal faulting events indicating extension of the landmasses occur on either side of the Aegean Sea, figure 1.

The extension observed on both sides of the Aegean Sea is accommodated by large east-west trending normal fault systems like the Gulf of Corinth in the West Aegean and Gediz Graben and Büyük Menderes Graben in the east. The change in the GPS velocity field from west to southwest occurs along the eastern Aegean close to the study area around Izmir.

The Mineral Research and Exploration Institute, Ankara, Turkey (MTA) has recently located more than 40 active faults in the vicinity of Izmir (Emre, et al., 2005). Aktug and Kiliçoglu (2006) have investigated the velocity field around İzmir more closely by a local GPS survey based on previous data (from 1992 and newer) and a new denser network (2001-2004). The geographical coverage of this network with special emphasis on three large faults in the area: the İzmir fault, the Gülbahçe fault and the Tuzla fault, figure 2, are referred to as scenario 1(A-C) IF, 2 GF and 3 TF, in this study. The detailed geographical coverage of the GPS network has the advantage

of being able to map small-scale block rotations instead of looking at the entire western Anatolia as one single rigid block. Also the network was set up in order to map the rate of opening and extension across the İzmir bay. The velocity field is given in figure 2 with respect to the Anatolian fixed reference frame. From the figure it is evident that block rotations exist in the area around İzmir; especially the relative velocities on each side of the Seferihisar and Tuzla faults are significant. The increase in velocities from east to west and north to south is also evident, like the change in the velocity field across the İzmir bay, which confirms the opening of the bay.

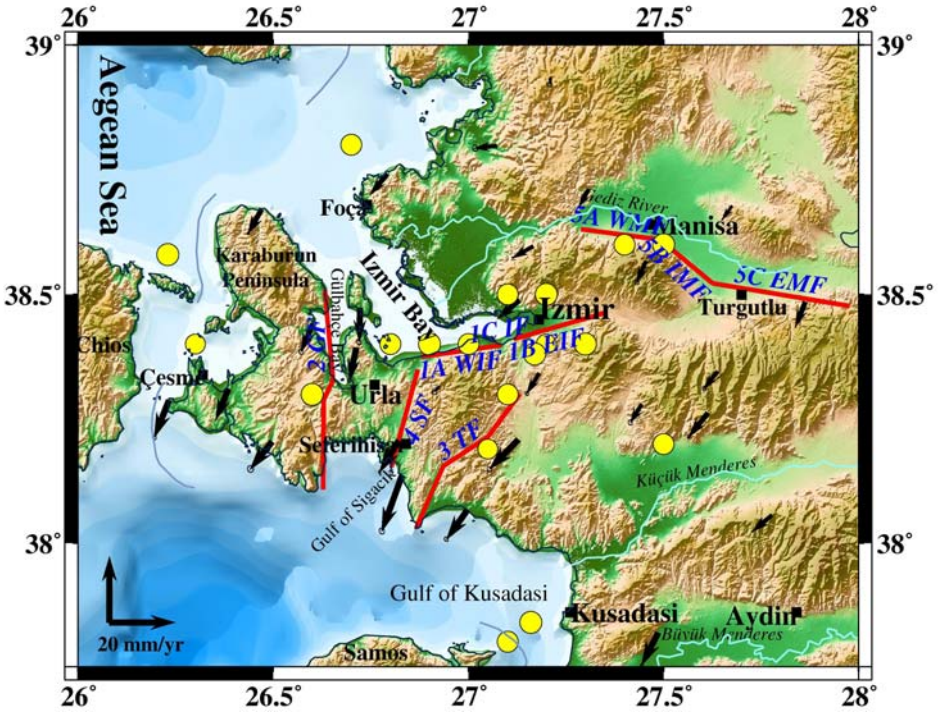

Figure 2 The GPS field in the vicinity of İzmir with a stable Anatolian block as a reference frame is shown with black arrows, from Aktug and Kilicoglu (2006). The historical earthquakes that have caused significant ground shaking in Izmir during 47-1992, are shown in yellow circles, from Papazachos et al. (1997), Papazachos and Papazachou (1997) and Ambraseys and Finkel (1995) and the faults for which ground motion simulations are conducted are shown as red lines. Scenario names are given in table 1.

Both on a regional scale, figure 1, and on a local scale tectonic deformation in western Anatolia produces a high rate of seismic activity. During historical times İzmir and its surroundings is known to have experienced several very destructive earthquakes, figure 2. From the macroseismic records compiled by Papazachos et al. (1997), Papazachos and Papazachou (1997) and Ambraseys and Finkel (1995) it is evident that the area surrounding İzmir has been subject to severe ground shaking and that the city has been destroyed several times. The historic events in figure 2 draw up a clear sign of activity on both the İzmir and the Tuzla faults. The latest large earthquake with hypocenter near İzmir occurred in 1788 with a moment magnitude of 6.4 following two earlier events in 1688 and 1723. During the last 220 years no large earthquake has taken place near the city, which indicates that there is built up a significant amount of stress on the faults surrounding the city.

Recently, in autumn 2005 a high seismic activity was observed in the Gulf of Sigacik with approximately 50 events (Mw >3) from the 17th to the 31st of October, and three earthquakes of moment magnitudes larger than 5.4 took place within three days (Aktar, et al., 2007). The focal mechanisms of the large events indicate a strike-slip motion on faults striking northeast southwest in the Gulf of Sigacik.

In this study seismic hazard in İzmir and the surrounding area is estimated based in ground motion simulations using earthquake rupture scenarios. These simulations are calculated for different frequency ranges, and the methodology follows the approach of Pulido and Kubo (2004) and Pulido et al. (2004). The low-frequency ground motion (0.1-1.0 Hz) is obtained by subdividing the fault plane into several subfaults that are treated as several independent point sources. The seismograms for the low-frequency motion are obtained numerically by the discrete wave number theory (Bouchon, 1981).The total ground motion is found by adding the different contributions assuming a constant rupture velocity within each subfault. This method computes the wave

propagation in a flat layered velocity structure for a given focal mechanism and source time function and is described below. The high frequency ground motion (1-10 Hz) is calculated from a finite asperity model as the case for the low frequency ground motion. The point source ground motions are calculated using a semi-stochastic approach (Boore, 1983). Finally the summation of the high-frequency ground motion for each point source is obtained by applying the empirical Greens function method (Irikura, 1986). The radiation pattern for low-frequency ground motion follows the theoretical double couple, whereas for the high-frequencies the radiation pattern is isotropic and spherical (Pitarka, et al., 2000). To be able to take the variation of the radiation pattern for SV and SH waves into account Pulido and Kubo (2004) developed a method, which gives a smooth transition from the low-frequency pattern to the high-frequency pattern. This hybrid approach for the ground motion simulations has previously been found to produce realistic results, (Pulido and Kubo, 2004; Pulido, et al., 2004; Sørensen, et al., 2007).

3. SCENARIO EARTHQUAKE PARAMETERS

In order to asses seismic hazard in Izmir nine earthquake scenarios are constructed on faults shown in figure 2 and the corresponding ground motions are computed. The rupture initiation point for all earthquake scenarios is chosen in order to produce worst-case scenarios for Izmir.

The crustal and upper mantle velocity model used in this study assumes a midcrustal low-velocity zone and a crust of 33 km (Horasan, et al., 2002). The attenuation of the simulated seismic waves of low frequency are determined from Q-values from the velocity model, while a frequency dependent attenuation relation is applied for the higher frequencies (Akinci, et al., 1995) up to 10 Hz.

Risetime is selected to be 1.0 s and 3.0 s for the scenarios on normal faults and strike-slip faults respectively. The rupture velocities are selected to be 2.5 and 3.0 km/s for the two fault types respectively (Pulido, et al., 2004; Somerville, et al., 1999).

The total size of the asperities is in previous studies found to be about 22% of the total ruptured area (Somerville, et al., 1999). In most of the scenario earthquakes of this study there is only one asperity per fault, and in the cases of several asperities an asperity size corresponding to 22% of the segment area has been adopted. This choice of the size of the individual asperities is consistent with previous studies where earthquake ground motion simulations have been conducted (Pulido and Kubo, 2004; Pulido, et al., 2004; Sørensen, et al., 2007).

Table 1 Source parameters for the nine different earthquake scenarios. The Izmir and Manisa faults are normal faults, while the three others are of strike-slip characteristics. Ground motion simulation were conducted for frequencies up to 10 Hz and with a frequency dependent attenuation of $Q = 82 \cdot f^{1.0}$. For Gülbahce and Tuzla faults the fault plane solutions are given as northern, mid and southern segment, while for scenario 1C they are given from the west to the east.

Scenario fault	Moment magnitude	Seismic moment (Nm)	Fault Plane Solution (strike/dip/rake)	Average stress drop (MPa)	Asperity stress drop (high-slip) (MPa)
1A W. Izmir	6.5	$6.2 \cdot 10^{18}$	263°/60° /-100°	3.0	11.6
1B E. Izmir	6.5	$8.2 \cdot 10^{18}$	257°/60° /-100°	3.0	11.6
1C Izmir	6.9	$2.3 \cdot 10^{19}$	263°/60° /-100° 250°/60° /-100° 257°/60° /-100°	3.0	11.6
2GF Gülbahce	6.9	$3.2 \cdot 10^{19}$	180°/80° /-10° 211°/80° /-10° 173°/80° /-10°	8.0	31.0
3TF Tuzla	6.9	$2.6 \cdot 10^{19}$	29°/80° /-167° 63°/80° /-167° 44°/80° /-167°	7.9	30.5
4SF Seferihisar	6.6	$1.1 \cdot 10^{19}$	199°/80° /-149°	7.9	28.8
5A W. Manisa	6.5	$6.2 \cdot 10^{18}$	276°/48° /-83°	3.0	11.6
5B I. Manisa	6.4	$4.5 \cdot 10^{18}$	304°/48° /-83°	3.0	11.6
5C E. Manisa	6.6	$9.2 \cdot 10^{18}$	277°/48° /-83°	3.0	11.6

The seismic moment for the different earthquake scenarios are determined from the moment magnitude applied to each scenario earthquake from the fault length (Kanamori, 1977; Wells and Coppersmith, 1994) where 40% is applied to the asperity (high-slip) and 60% to the background fault plane (low-slip). The average stress

drop is for the scenarios in the normal faults determined to be 3.0 MPa (Tselentis and Zahradnik, 2000). For the scenarios on the strike-slip faults the stress drop is found from the seismic moment (Das and Kostrov, 1986). Stress drop ratio between the asperities and background of the fault plane is assumed 0.05 (Dalguer, et al., 2004). All simulation parameters are summarized in table 1.

4. GROUND MOTION SIMULATION RESULTS

The peak ground motion (PGM) values for the nine different earthquake scenarios and the duration of the signals as simulated for the center of Izmir are given in table 2. Here peak ground motion values are given both scenario wise and simulated for a station in the center of Izmir. It is obvious that the simulations of the three strike-slip scenarios produce the highest peak ground accelerations (PGA), whereas the scenario of the entire Izmir fault (42 km long) produces the highest peak ground velocity (PGV) and also a very high value for the PGA. The fact that the scenario on the Seferihisar fault with moment magnitude of 6.6 produces larger ground motions than the earthquake scenario with moment magnitude 6.9 on the Izmir fault (1C) is consistent with previous studies: that larger ground motions are to be expected on strike-slip faults than on normal faults (Brune and Anooshehpoor, 1999; Mcgarr, 1984).

Table 2 Output values for peak round acceleration and velocity (PGA and PGV) scenario wise and as simulated in the center of Izmir. Signal duration is for the station in the center of Izmir.

Earthquake scenario	PGA scenario (cm/s^2)	PGV scenario (cm/s)	PGA Izmir (cm/s^2)	PGV Izmir (cm/s)	Signal duration (Izmir) (s)
1A W. Izmir	256	35	144	10	5
1B E. Izmir	262	28	227	24	7
1C Izmir	438	68	387	53	13
2GF Gülbahce	559	40	125	6	11
3TF Tuzla	574	47	253	13	6
4SF Seferihisar	526	32	94	3	12
5A W. Manisa	255	26	56	7	8
5B I. Manisa	209	12	35	3	11
5C E. Manisa	274	29	21	3	11

The estimation of the seismic hazard in Izmir is based on computed waveforms from each scenario for a station located in the center of Izmir. The PGM values and duration of the signals are given in table 2. These values show that the earthquake scenarios on the Izmir fault (1C) and Tuzla fault produce the largest ground motions in Izmir, and the duration of the signal on the Izmir fault is the longest simulated. From this it is evident that the energy reaching Izmir from these scenarios is much larger than for the other earthquake scenarios. They are consequently considered the worst-case scenarios for Izmir regarding seismic hazard. The distribution of PGM for the scenario earthquakes on these faults are shown in figure 3. Obviously the high values of peak ground motions observed in İzmir for scenario 1B EIF and 1C IF are partly explained by the proximity of the site to the scenario faults. In such cases the effect of attenuation is at minimum.

The simulation results for the nine earthquake scenarios have been compared to five different empirical attenuation relations for PGAs and PGVs (Akkar and Bommer, 2007; Ambraseys, et al., 1996; Campbell, 1997; Gülkan and Kalkan, 2002; Pankow and Pechmann, 2004; Spudich, et al., 1997). For the simulation on the Tuzla fault this is in figure 4 shown for distances up to 400 km from the fault. All empirical relations are set up with hard rock conditions, since ground motions were simulated for the bedrock. These results yield that the simulated values for the PGA fit very well with the empirical attenuation relations. For distances of less than 30 kilometers to the fault, however, the PGAs are higher than the attenuation relations predict. For the PGVs the simulated values have a larger spread, but the simulation results lie in the range predicted by the different empirical attenuation relations, though there is a tendency for the simulated PGV values to be in the higher range of the of the empirical relations, especially at larger distances. In respect of the simulations for normal fault earthquakes the simulated ground motions will generally be a bit lower than the empirical relations; which is as previously explained again consistent with the experience of lower ground motions for earthquakes on normal faults compared to strike-slip events. Generally there seems to be a reasonably good agreement between the simulated ground motions and empirical predictions.

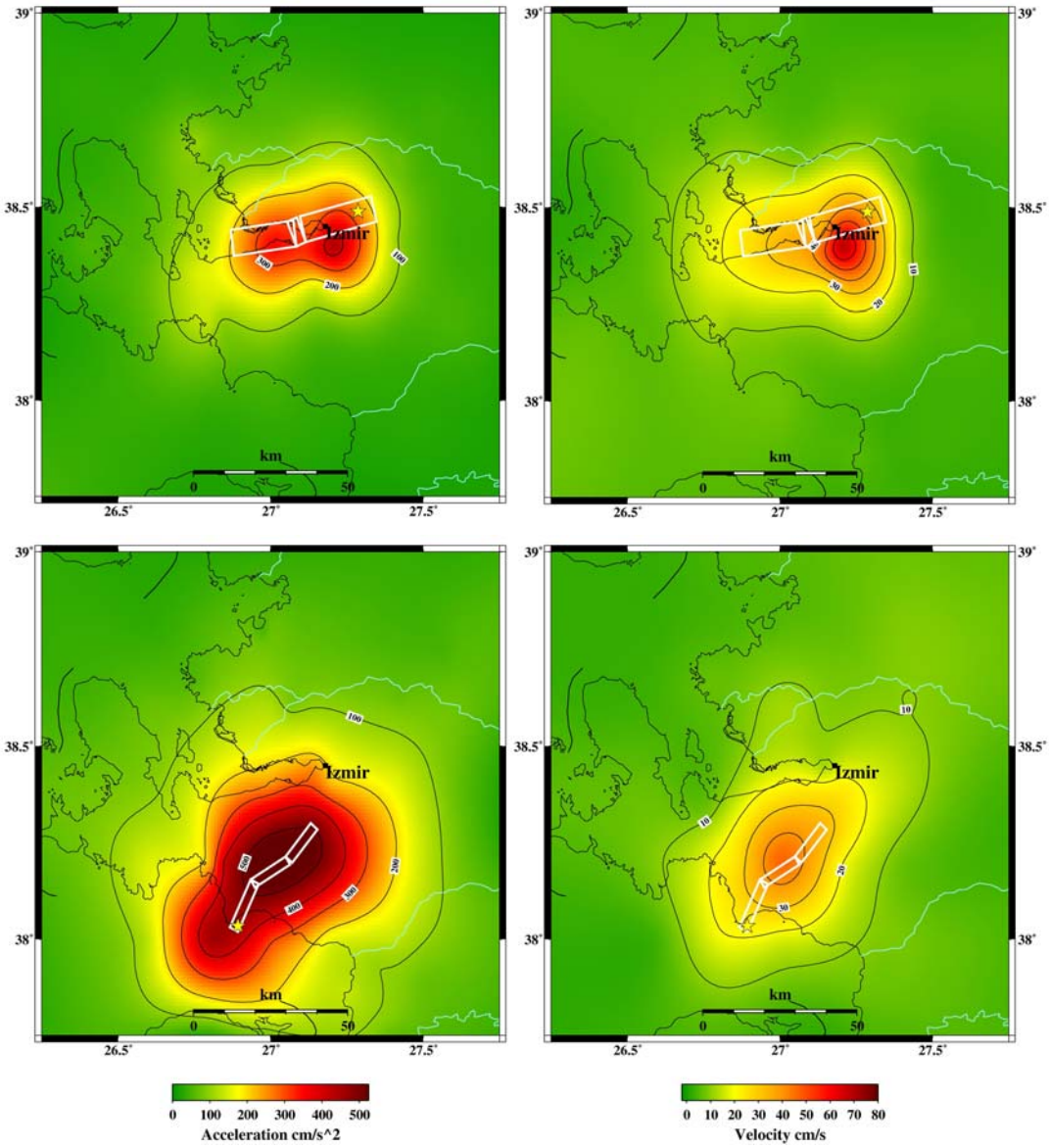

Figure 3 PGA (left) and PGV (right) distribution for earthquake scenario 1C Izmir fault (top) and 3TF Tuzla fault (bottom).

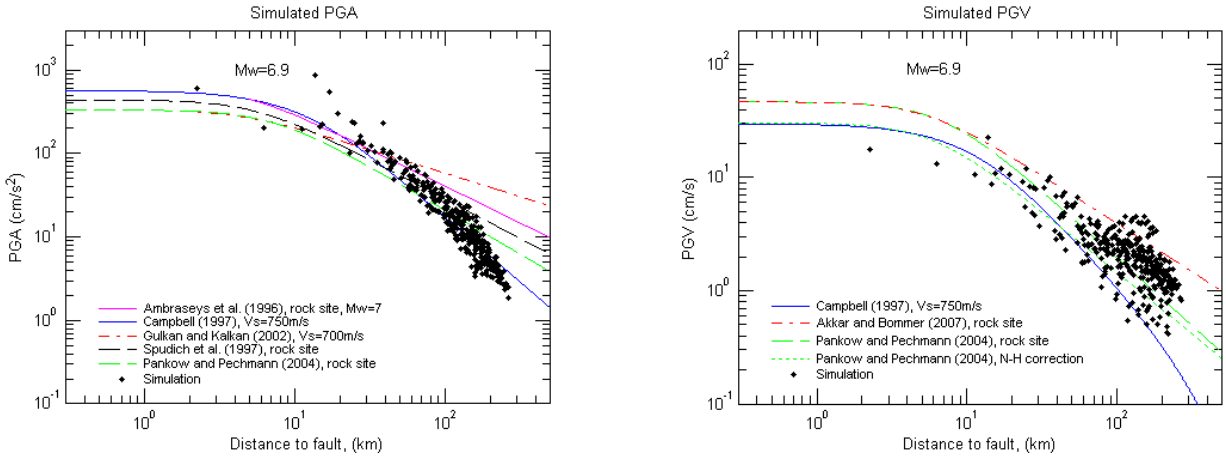

Figure 4 Comparison of simulated (black dots) peak ground acceleration (left) and velocity (right) to ground motions predicted by the empirical attenuation relations mentioned in the text. The comparison is made with the results obtained for the earthquake scenario 3 TF, Tuzla fault.

The velocity response spectra for the nine scenario earthquakes at the station in İzmir center are shown in figure 5. For all scenarios, except those on the different fault segments of the İzmir fault, very low spectral velocity values are seen, with no major peaks. There are, however, minor peaks on the spectra from the earthquake scenario 3 TF on Tuzla Fault (green) for frequencies between 0.1 to 0.4 Hz on both horizontal components. The absolute spectral velocity values, on the other hand, are only in the range of 25 cm/s in these peaks. The dominating earthquake scenarios in figure 5 are those simulated on the different İzmir fault segments (blue). Especially for the scenarios 1B EIF (stippled line) and 1C IF (solid line) strong peaks are observed in the frequency range of 0.2 to 1 Hz. The peaks are strongest for scenario 1C IF, on the combined rupture of the two segments, while they are weakest for the scenario on the westernmost segment, 1A. The peaks on the vertical component for scenario 1A-C IF indicate a vertical displacement during the rupture in agreement with the normal faulting mechanisms of these scenarios.

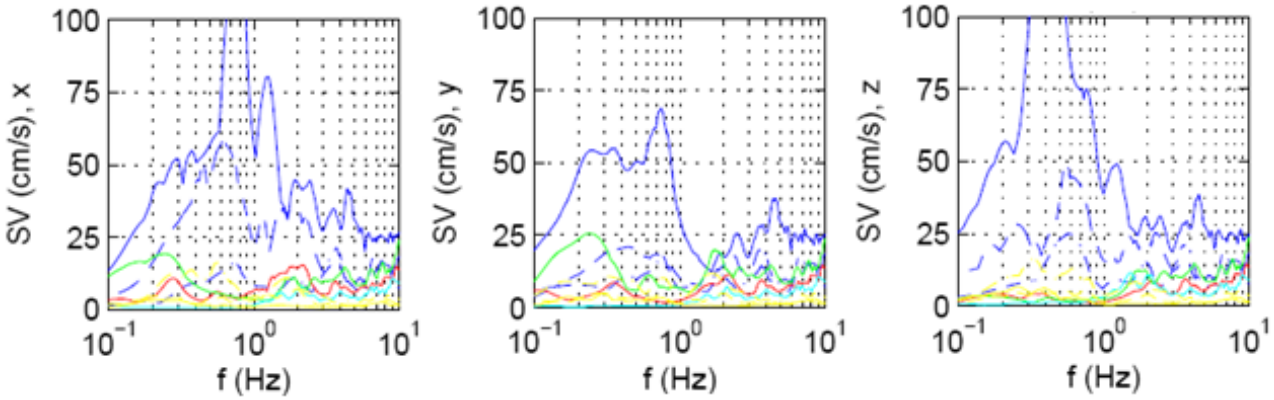

Figure 5 Comparison of the velocity response spectra for all nine scenarios. Scenario 1A-C (blue):1A (dotted stippled) 1B (stippled) and 1C (solid) and 3 TF (green). The horizontal components are given as x for east-west and y for north-south, z is the vertical component.

In this study all ground motion simulations are conducted for bedrock conditions and hence the possible local site effects are not taken into account. Due to the north-south extension in western Anatolia large graben structures are developed. The origin of the İzmir bay is associated with similar extensional tectonics and results in basin development in time. The current morphology in the area clearly indicates two distinct features. The areas located topographically high are associated with the bedrock outcrops, whereas the low-lying areas represent the accumulated sedimentary deposits. The large part of the metropolitan area of İzmir is situated on such sedimentary deposits. Furthermore, the significant fluvial deposition occurs in the delta of the Gediz River in the northern part of the İzmir Bay. Comparing the fundamental frequency range found in a previous study (Atakan, 2005) with frequencies where peaks are observed in the response spectra (figure 5) from the earthquake scenarios on the İzmir fault leads to the evident conclusion that there is an overlap in the frequency range. The modeled ground motions are thus expected to amplify significantly in this frequency range.

5. CONCLUSIONS

In this study ground motion caused by nine earthquake scenarios on faults in the vicinity of İzmir are conducted. It was found that the worst-case scenario for seismic hazard in the center of İzmir is scenario 1C IF. Peak ground accelerations of 291 cm/s2 and peak ground velocities of 48 cm/s are estimated. The frequency content of the simulated response spectra is in the same frequency range found for the fundamental frequency for sites in İzmir in a previous H/V study, suggesting significant potential site effects due to amplification.

The attenuation relation used in the ground motion simulations agrees well with empirical relations in case of the peak ground accelerations for the scenarios conducted for strike-slip faulting earthquakes; whereas the simulated values obtained for the normal faulting earthquakes are found to be lower than predicted. Finally it was found that the earthquake scenarios conducted on the three segments of the Manisa fault (scenario 5A-C) are considered to be of marginal concern with regard to the hazard in İzmir.

REFERENCES

Akinci, A., Ibanez, J.M., Del Pezzo, E. and Morales, J. (1995). Geometrical spreading and attenuation of Lg waves: a comparison between western Anatolia (Turkey) and southern Spain. *Tectonophysics* **250:1**, 47-60.

Akkar, S. and Bommer, J.J. (2007). Empirical Prediction Equations for Peak Ground Velocity Derived from Strong-Motion Records from Europe and the Middle East. *Bulletin of the Seismological Society of America* **97:2**, 511-530.

Aktar, M., Karabulut, H., Özalaybey, S. and Childs, D. (2007). A conjugate strike-slip fault system within the extensional tectonics of Western Turkey. *Geophysical Journal International* **171:**1363-1375.

Ambraseys, N., Simpson, K. and Bommer, J. (1996). Prediction of horizontal response spectra in Europe. *Earthquake engineering and structural dynamics* **25:**371-400.

Ambraseys, N.N. and Finkel, C.F. (1995), The Seismicity of Turkey and Adjacent Areas, A Historical Review, 1500-1800, Muhittin Salih EREN, Istanbul.

Boore, D.M. (1983). Stocastic simulation of high-frequency ground motions based on seismological models of the radiated spectra. *Bulletin of the Seismological Society of America* **73:6**, 1865-1894.

Bouchon, M. (1981). A simple method to calculate Green's functions for elastic layered media. *Bulletin of the Seismological Society of America* **71:4**, 959-971.

Brune, J.N. and Anooshehpoor, A. (1999). Dynamic geometrical effects on strong ground motion in a normal fault model. *Journal of Geophysical Research* **104:B1**, 809-815.

Campbell, K.W. (1997). Empirical Near-Source Attenuation Relationships for Horizontal and Vertical Components of Peak Ground Acceleration, Peak Ground Velocity, and Pseudo-Absolute Acceleration Response Spectra. *Seismological Research Letters* **68:1**, 154-179.

Gülkan, P. and Kalkan, E. (2002). Attenuation modeling of recent earthquakes in Turkey. *Journal of Seismology* **6:**397-409.

Horasan, G., Gulen, L., Pinar, A., Kalafat, D., Ozel, N., Kuleli, H.S. and Isikara, A.M. (2002). Lithospheric Structure of the Marmara and Aegean Regions, Western Turkey. *Bulletin of the Seismological Society of America* **92:1**, 322-329.

Kanamori, H. (1977). The energy release in great earthquakes. *Journal of Geophysical Research* **82:B20**, 2981-2988.

Mcgarr, A. (1984). Scaling ground motion parameters, state of stress, and focal depth. *Journal of Geophysical Research* **89:**6,969-6979.

Nyst, M. and Thatcher, W. (2004). New constraints on the active tectonic deformation of the Aegean. *Journal of Geophysical Research* **109:B11**, 406-430.

Pankow, K.L. and Pechmann, J.C. (2004). The SEA99 Ground-Motion Predictive Relations for Extensional Tectonic Regimes: Revisions and a New Peak Ground Velocity Relation. *Bulletin of the Seismological Society of America* **94:1**, 341-348.

Papazachos, B. and Papazachou, C. (1997), The Earthquakes of Greece, *Technical books Edition*, **Thessaloniki**.

Papazachos, B.C., Papaioannou, C.A., Papazachos, C.B. and Savvaidis, A.S. (1997), Atlas of Isoseismal Maps for Strong Shallow Earthquakes in Greece and Surrounding Area (426BC-1995), *Technical books Editions*, **Thessaloniki**.

Pitarka, A., Somerville, P., Fukushima, Y., Uetake, T. and Irikura, K. (2000). Simulation of Near-Fault Strong-Ground Motion Using Hybrid Green's Functions. *Bulletin of the Seismological Society of America* **90:3**, 566-586.

Pulido, N. and Kubo, T. (2004). Near-fault strong motion complexity of the 2000 Tottori earthquake (Japan) from a broadband source asperity model. *Tectonophysics* **390:1-4**, 177-192.

Pulido, N., Ojeda, A., Atakan, A. and Kubo, T. (2004). Strong ground motion estimation in the Sea of Marmara region (Turkey) based on a scenario earthquake. *Tectonophysics* **391:**357-374.

Somerville, P., Irikura, K., Graves, R., Sawada, S., Wald, D., Abrahamson, N., Iwasaki, Y., Kagawa, T., Smith, N. and Kowada, A. (1999). Characterizing Crustal Earthquake Slip Models for the Prediction of Strong Ground Motion. *Seismological Research Letters* **70:,** 59 - 80.

Spudich, P., Fletcher, J.B., Hellweg, M., Boatwright, J., Sullivan, C., Joyner, W.B., Hanks, T.C., Boore, D.M., Mcgarr, A., Baker, L.M. and Lindh, A.G. (1997). SEA96 - A New Predictive Relation for Earthquake Ground Motions in Extensional Tectonic Regimes. *Seismological Research Letters* **68:1**, 190-198.

Sørensen, M.B., Atakan, K. and Pulido, N. (2007). Simulated Strong Ground Motions for the Great M 9.3 Sumatra-Andaman Earthquake of 26 December 2004. *Bulletin of the Seismological Society of America* **97:1A**, S139-151.

Tselentis, G.A. and Zahradnik, J. (2000). The Athens Earthquake of 7 September 1999. *Bulletin of the Seismological Society of America* **90:5**, 1143-1160.

Wells, D.L. and Coppersmith, K.J. (1994). New empirical relationships among magnitude, rupture length, rupture width, rupture area, and surface displacement. *Bulletin of the Seismological Society of America* **84:4**, 974-1002.